Prostatic cancer surveillance following whole-gland high-intensity focused ultrasound: comparison of MRI and prostate-specific antigen for detection of residual or recurrent disease

[1]S PUNWANI, FRCR, PhD, [2]M EMBERTON, FRCS, [1]M WALKDEN, FRCR, [3]A SOHAIB, FRCR, [4]A FREEMAN, FRCP, ^{2}H AHMED, FRCS, [1]C ALLEN, FRCR and [1]A KIRKHAM, FRCR

[1]Department of Radiology, University College London Hospital, London, UK, [2]Department of Urology, University College London Hospital, London, UK, [3]Department of Imaging, Royal Marsden Hospital, London, UK, and [4]Department of Pathology, University College London Hospital, London, UK

Objective: This retrospective study compares dynamic contrast-enhanced (DCE) MRI with the serial prostate-specific antigen (PSA) measurement for detection of residual disease following whole-gland high-intensity focused ultrasound (HIFU) therapy of prostate cancer.

Methods: Patients in whom post-HIFU DCE-MRI was followed within 3 months by ultrasound-guided transrectal biopsy were selected from a local database. 26 patients met the study inclusion criteria. Serial PSA levels following HIFU and post-HIFU follow-up MRI were retrieved for each patient. Three radiologists unaware of other investigative results independently assessed post-HIFU MRI studies for the presence of cancer, scoring on a four-point scale (1, no disease; 2, probably no disease; 3, probably residual disease; and 4, residual disease). Sensitivity, specificity and receiver operating characteristic (ROC) analysis were performed for each reader, post-HIFU PSA nadir and pre-biopsy PSA level thresholds of >0.2 and $>0.5 \, \mathrm{ng \, ml^{-1}}$.

Results: The sensitivity of DCE-MRI for detection of residual disease for the three readers ranged between 73% and 87%, and the specificity between 73% and 82%. There was good agreement between readers ($\kappa = 0.69$–0.77). The sensitivity and specificity of PSA thresholds was 60–87% and 73–100%, respectively. The area under the ROC curve was greatest for pre-biopsy PSA (0.95).

Conclusion: DCE-MRI performed following whole-gland HIFU has similar sensitivity and specificity and ROC performance to serial PSA measurements for detection of residual or recurrent disease.

High-intensity focused ultrasound (HIFU) is a promising alternative management paradigm for prostate cancer available to patients with organ-confined disease. Whole-gland treatment is achievable while sparing the neurovascular bundles and external urethral sphincter [1, 2]. As a result, reported rates of urinary and sexual morbidity are lower and quality of life higher following HIFU therapy than following radical prostatectomy [3].

However, recurrence rates as high as between 30% and 40% at 5 years have been reported [4]. Identification of potential residual or recurrent disease is therefore paramount, guiding administration of salvage therapy [5]. Accepted surveillance for residual or recurrent tumour following whole-gland HIFU is reliant on serial prostate-specific antigen (PSA) measurements followed by biopsy for patients with a high or rising PSA [6].

There are several potential advantages of assessing post-HIFU residual disease with MRI. First, MRI may provide a more sensitive test than PSA, as it is able to detect disease not elevating PSA but causing a change in the MRI features of residual prostatic tissue. Second, when disease is detected on MRI, it is clear that imaging also provides the location of disease and therefore has the added advantage of being able to guide biopsy and salvage therapy. Finally, as primary focal treatment (*e.g.* hemi-ablation) of prostate cancer becomes established [7], it is highly likely that identification of residual disease by PSA alone will become more difficult, as PSA from untreated prostate may mask residual disease. Development of an imaging-based alternative for detection of residual or recurrent disease in the post-HIFU prostate is therefore necessary.

Dynamic contrast-enhanced (DCE) MRI has been used for detection of cancer in the untreated prostate, and has performance characteristics similar to gland biopsy [8]. DCE-MRI has also been reported to detect residual disease after radiotherapy [9]. Moreover, early studies investigating DCE-MRI in patients treated with whole-gland HIFU have shown promising results for detection of residual tumour [6, 10].

Our study assesses the performance of DCE-MRI to detect residual or recurrent disease in the post-HIFU (whole-gland) prostate, and compares this with serial PSA measurement.

Address correspondence to: Dr Alex Kirkham, Department of Radiology, 2nd Floor Podium, University College London Hospital, 235 Euston Road, London NW1 2BU, UK. E-mail: alexkirkham@yahoo.com

Methods and materials

Local ethics committee permission was obtained for use of retrospective patient data. Requirement for written consent was waived for this study.

A single observer searched a local database for patients with organ-confined prostate cancer treated with whole-gland HIFU using the Sonablate 500 (Focus Surgery, Indianapolis, IN) device between May 2005 and October 2007. Patients in whom post-treatment DCE-MRI was followed within 3 months by an ultrasound-guided transrectal biopsy were selected for inclusion. 26 patients (median age 62 years, range 47–80 years) met all inclusion criteria (representing approximately 27% of the total data set). Clinical details for individual patients are given in Table 1.

A ''standards for the reporting of diagnostic accuracy studies'' (STARD) flow diagram for this study is illustrated in Figure 1.

Whole-gland high-intensity focused ultrasound treatment

All included patients underwent treatment using the whole-gland HIFU technique as previously described [11, 12].

In brief, therapy was administered under general anaesthesia with patients in the lithotomy position using an endorectal HIFU probe. Treatment was planned using ultrasound-acquired volumes consisting of stacks of both sagittal and transverse sections (voxel size, $2 \times 3 \times 30$ mm) and was applied in rows that extended in the craniocaudal axis, interleaved to avoid interference from adjacent, recently treated areas.

MRI protocol

Follow-up MRI was performed a median of 6.6 months (range 5–20 months) after the initial HIFU treatment. Images were acquired on a Siemens 1.5 T system (Avanto; Siemens, Erlangen, Germany) using the manufacturer's pelvic phased array coil. Small field of view T_2 weighted rapid acquisition with relaxation enhancement (RARE) images were acquired in the axial and coronal planes. Axial fat-saturated T_1 weighted gradient echo images were obtained prior to contrast administration. A single dose (20 ml) of gadopentate dimeglumine (Magnevist; Schering, Berlin, Germany) was injected into an arm vein at $3\,\mathrm{ml\,s}^{-1}$ and dynamic (16 s temporal resolution) fat-saturated T_1 weighted imaging repeated for a total acquisition time of 9 min 20 s (Table 2).
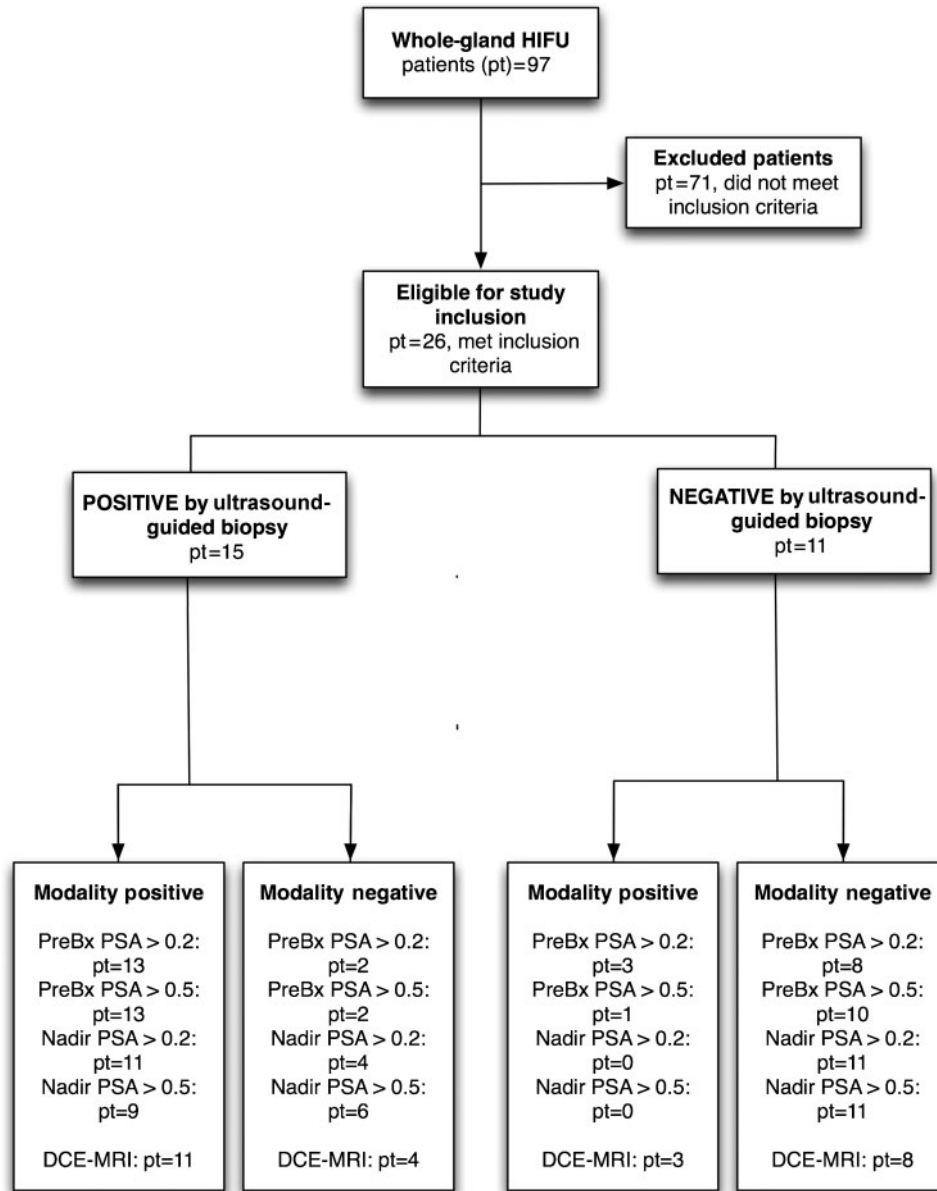
Prostate-specific antigen

All patients had PSA levels measured before and at 1.5, 3 and 6 months after HIFU therapy, and at a variable time interval after that. The median follow-up period was 17 months (range 6–30 months). The PSA nadir was

Table 1. Patient demographics and prostate-specific antigen and histology results after high-intensity focused ultrasound

Patient number	Age (years)	Pre-treatment Gleason grade	Time between HIFU and follow-up MRI (days)	Time between follow-up MRI and post-HIFU biopsy (days)	PSA nadir (ng ml^{-1})	PSA before biopsy (ng ml^{-1})	Post-treatment biopsy positive? Number of cores out of total (maximum cancer core length)
01[a]	47	3+3	173	1	0.11	0.11	Negative
02[a]	47	3+3	198	0	0	0.1	1/8 (<1 mm)
03[a]	52	4+3	225	0	0.45	0.51	2/10 (1 mm)
04[a]	53	3+3	165	36	0	0	Negative
05[a]	56	3+3	205	19	0	0	Negative
06[a]	58	3+4	167	42	0.51	0.92	2/10 (6 mm)
07	58	3+4	307	0	0.11	1.12	2/8 (1 mm)
08	57	3+4	647	1	0.11	0.5	Negative
09[a]	58	3+3	189	15	0	0	Negative
10[a]	59	3+4	184	16	0	0	Negative
11[a]	60	3+4	205	20	0.07	0.2	1/3 (1 mm)
12[a]	61	3+3	175	17	0	0	Negative
13[a]	60	3+3	158	23	0.16	0.34	Negative
14	61	3+3	367	0	0.2	0.6	Negative
15	65	3+4	220	3	0.94	1.16	1/4 (3 mm)
16[a]	64	3+3	190	13	0	0	Negative
17	66	3+3	211	29	1.2	3.8	4/4 (3 mm)
18	67	3+3	200	2	1.68	3.56	2/7 (1 mm)
19[a]	66	3+2	171	17	0	0	Negative
20	67	4+3	305	6	0	1.27	2/5 (1 mm)
21[a]	69	3+3	181	12	1.29	1.54	3/10 (1 mm)
22	68	3+4	604	0	0.29	1.4	3/8 (4 mm)
23	70	3+3	149	82	1.28	1.28	1/8 (<1 mm)
24	71	3+3	200	0	1.2	1.4	3/8 (4 mm)
25	74	3+4	449	1	0.9	1.7	2/8 (8 mm)
26	80	4+5	295	53	0.94	3.11	2/8 (1 mm)

HIFU, high-intensity focused ultrasound; PSA, prostate-specific antigen (0 signifies <0.05 ng ml^{-1}).
[a]Patients enrolled as part of a trial involving post-HIFU biopsy irrespective of PSA.

Figure 1. Standards for the reporting of diagnostic accuracy studies (STARD) study flow diagram. DCE, dynamic contrast-enhanced; HIFU, high-intensity-focused ultrasound; PreBx, pre biopsy; PSA, prostate-specific antigen.

defined as the lowest recorded value during the follow-up period.

Ultrasound-guided prostate biopsy

The indication for ultrasound-guided biopsy was a high post-HIFU PSA nadir or rising PSA level for 12 patients. The remaining 14 patients had biopsy performed irrespective of PSA level as part of the protocol for a separate prospectively running clinical trial. For both patient populations MRI had been clinically reported by a uroradiologist at our institution experienced in MRI of the prostate (CA, 15 years; AK, 5 years).

All patients' biopsies were performed by the same uroradiologists where appropriate using MRI to guide targeting of suspicious lesions. In addition, biopsies were distributed symmetrically across the remainder of the

gland to provide complete sampling. A median of eight cores (range two to ten) were obtained per patient, the exact number dependent on residual prostatic volume.

The median time between MRI and biopsy was 13 days (range 0–82 days). Histological presence or absence of residual disease was recorded.

MRI analysis

Image analysis was conducted on an IMPAX ES (Agfa-Gevaert, Mortsel, Belguim) PACS workstation. Post-treatment RARE and DCE-MRI studies with identifying information removed were evaluated independently by three radiologists experienced in prostate MRI reporting (MW, 1 year; AS, 5 years; and SP, 2 years of experience). Prior to assessment each reader was given the same 1 h tutorial by an experienced uroradiologist (AK)

Table 2. MRI sequence parameters

Parameter	T_2 weighted TSE	T_1 weighted 3D FLASH
TR (ms)	7500	10.4
TE (ms)	92	4.7
Flip angle (degrees)	180	15
Imaging plane	Axial/coronal	Axial
Slice thickness (mm)	3	3
Matrix	230×256	159×256
Field of view (mm)	180×180	260×260
Total acquisition time	6 min 24 s (per sequence)	9 min 20 s (including three 16 s pre-contrast scans)

3D, three-dimensional; FLASH, fast low-angle shot; TE, echo time; TR, repetition time; TSE, turbo spin echo.

on identification of residual disease on post-HIFU MRI. Tutorial images were specifically selected by the uro-radiologist from MRI examinations performed outside the study inclusion dates, thereby ensuring no patient overlap. Three MRI patterns were described at the tutorial based upon previous work [12]:

- Pattern 1: a low-volume, uniformly low-signal residual prostate, with no focus of early enhancement—in favour of no disease (Figure 2).

- Pattern 2: some residual prostate of mixed signal on T_2 weighted images with patchy low-level early enhancement—equivocal (Figure 3).
- Pattern 3: some residual prostate with a discrete enhancing focus—in favour of residual disease (Figure 4).

The three readers were aware that all patients had undergone whole-gland HIFU treatment for proven prostate cancer, but unaware of the results of previous

(a)

(b)

(c)
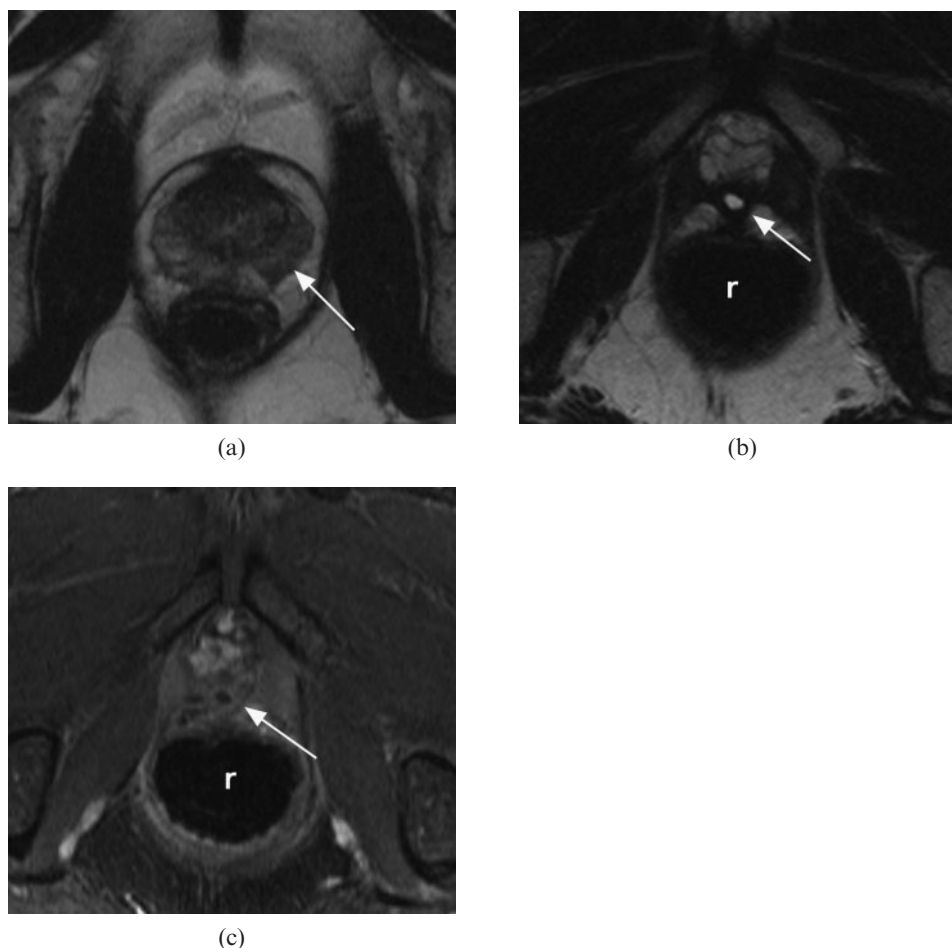
Figure 2. Residual tumour absent: axial T_2 weighted MR images (a) prior to and (b) following whole-gland high-intensity focused ultrasound therapy. (c) Post-therapy T_1 weighted contrast-enhanced image matched to (b). White arrow indicates the tumour location on the pre-treatment image (a) and the matched post-treatment location of expected recurrent tumour (b and c). r, rectum.

(a)

(b)

(c)
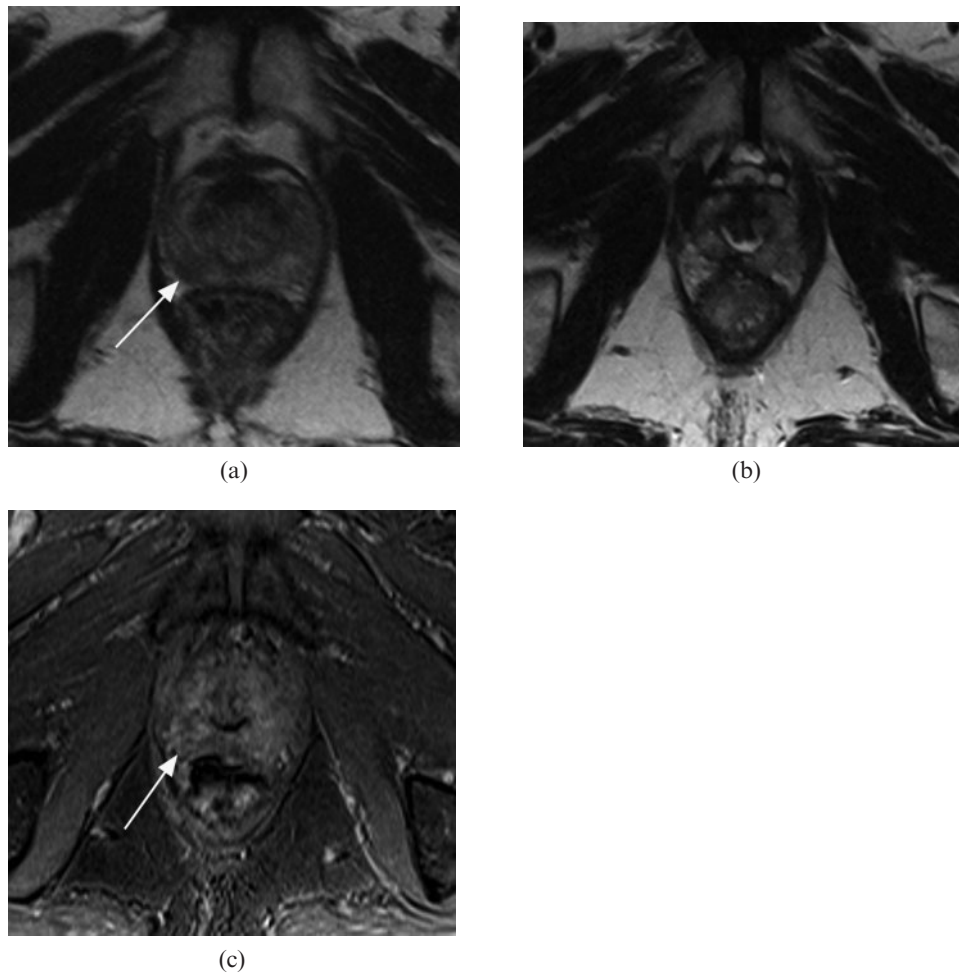
Figure 3. Equivocal appearances: axial T_2 weighted MR images (a) prior to and (b) following whole-gland high-intensity focused ultrasound therapy. (c) Post-therapy T_1 weighted contrast-enhanced image matched to (b). White arrow indicates the tumour location on the pre-treatment image (a) and the matched post-treatment location of expected recurrent tumour (c).

MRI studies, pre-treatment disease location, patient-specific clinical information and whether they were part of the clinical trial. Each reader scored the prostate for the presence or absence of disease using a four-point scale (1, no disease; 2, probably no disease; 3, probably residual disease; and 4, residual disease).

Statistical analysis

All data analyses were performed using SPSS version 18 (IBM Corporation, Armonk, NY).

The sensitivity and specificity for detection of residual disease was calculated for each reader using ultrasound-guided biopsy as a reference standard. For calculation, reader scores of 1 and 2 were considered negative and scores of 3 and 4 positive for disease. In addition, the majority opinion (of the three independent readers) on the presence or absence of disease was used to derive a consensus score.

Sensitivity and specificity of PSA thresholds of >0.2 and >0.5 $ng\,ml^{-1}$ applied to post-HIFU pre-biopsy PSA and PSA nadir values were also calculated.

Agreement between individual readers for identification of residual disease was calculated using κ statistics

[13]. A κ-value <0.2 was considered to indicate poor agreement; 0.2 to <0.4, fair agreement; 0.4 to <0.6, moderate agreement; 0.6 to <0.8, good agreement; and 0.8–1.0, very good agreement.

A receiver operating characteristic (ROC) curve was generated for each reader and PSA threshold. Area under the curve (AUC) was calculated and compared between ROC curves by the method described by Hanley and McNeil [14].

Results

Results for individual diagnostic methods are presented in the STARD flow chart (Figure 1). Ultrasound-guided biopsies performed following HIFU were positive for 15 of the 26 (58%) patients.

Mean post-HIFU PSA nadir was 0.72 (SD $\pm$0.55) and 0.05 (SD $\pm$0.08) $ng\,ml^{-1}$; and mean post-HIFU pre-biopsy PSA 1.54 (SD $\pm$1.12) and 0.14 (SD $\pm$0.23) $ng\,ml^{-1}$ for ultrasound-guided biopsy positive and negative patients, respectively. There was a significant difference between ultrasound-guided biopsy positive and negative patients' post-HIFU PSA nadir and also post-HIFU pre-biopsy PSA level ($p=0.01$ and $p<0.01$, respectively).

(a)

(b)

(c)
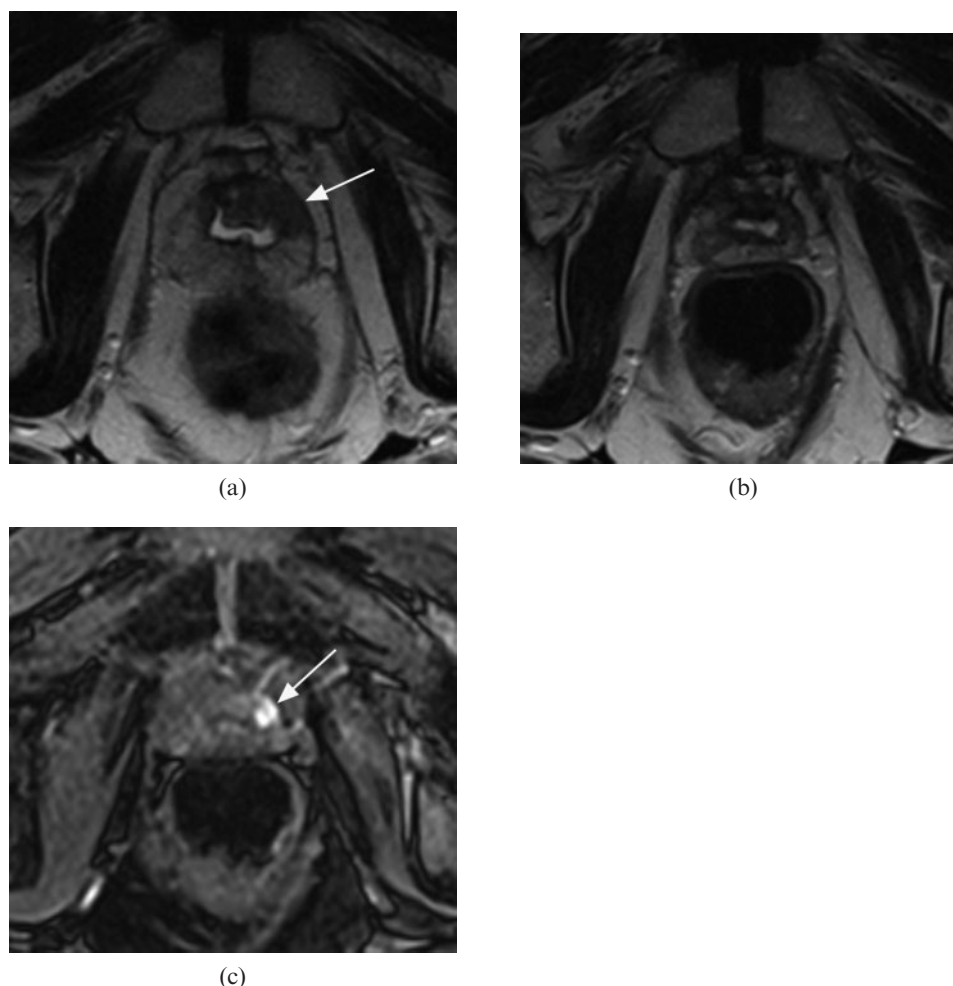
Figure 4. Residual tumour present: axial T_2 weighted MR images (a) prior to and (b) following whole-gland high-intensity focused ultrasound therapy. (c) Post-therapy T_1 weighted contrast-enhanced image matched to (b). White arrow indicates the tumour location on the pre-treatment image (a) and the matched post-treatment location of recurrent tumour (c).

The sensitivity and specificity of the post-HIFU pre-biopsy PSA for detection of residual disease was 87% and 73%; and 87% and 91% for PSA threshold values of $>0.2\,\mathrm{ng\,ml}^{-1}$ and $>0.5\,\mathrm{ng\,ml}^{-1}$, respectively. The sensitivity and specificity for the post-HIFU PSA nadir was 73% and 100%, and 60% and 100% for PSA threshold values of $>0.2\,\mathrm{ng\,ml}^{-1}$ and $>0.5\,\mathrm{ng\,ml}^{-1}$, respectively.

The sensitivity and specificity of individual readers for detection of residual disease using DCE-MRI was 87% and 73% (Reader 1), 73% and 82% (Reader 2) and 80% and 73% (Reader 3). There was good agreement between readers on the presence or absence of disease ($\kappa=0.69$–0.77). For the consensus scores, sensitivity and specificity of DCE-MRI for detection of residual disease was 73% and 73%, respectively.

ROC curves for the post-HIFU PSA nadir (AUC=0.87) and post-HIFU pre-biopsy PSA (AUC=0.95) are illustrated in Figure 5. ROC curves for individual readers are depicted in Figure 6. The AUC of the ROC curves for Readers 1, 2 and 3 was 0.87, 0.83 and 0.83, respectively.

The AUC of PSA methods (both nadir and pre-biopsy) was greater than the AUC of individual DCE-MRI readers, reaching borderline statistical significance ($p=0.05$–0.10). There was no significant difference between other ROC AUC comparisons.

Of the 11 patients who had negative transrectal biopsy after HIFU, all are now at least 3 years after treatment. 10 have a PSA persistently $<0.5\,\mathrm{ng\,ml}^{-1}$ and have not required retreatment. One patient had no evidence of disease on the initial MRI, and was negative at biopsy. However, a rising PSA (to $1.2\,\mathrm{ng\,ml}^{-1}$) 2 years after treatment prompted a further MRI. This showed a focus of tumour at the base, close to the seminal vesicle angle, confirmed by targeted biopsy and treated by HIFU.

Discussion

We usually perform MRI following HIFU at two discrete times: early (less than a month) after treatment to assess necrosis [12] (useful for feedback to the operator, but not the subject of this paper) and late (after 6 months) for the detection of recurrent disease. Images obtained in the interval between the two are often difficult to interpret, with residual disease easily masked by the enhancing rim surrounding the resolving necrotic focus [12]. At approximately 6 months following HIFU, necrotic tissue and its associated rim enhancement are replaced by fibrosis. Focal intense enhancement seen on DCE-MRI at this time is believed to represent residual or recurrent cancer.
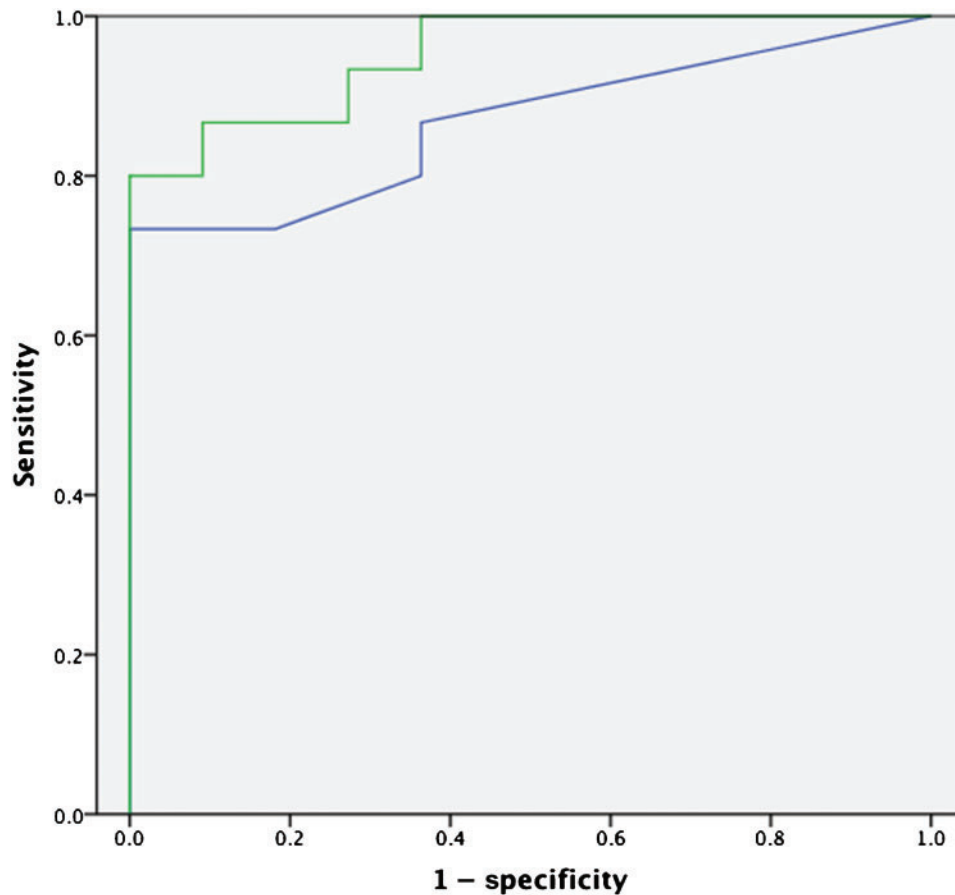
Figure 5. Receiver operating characteristic curves for post high-intensity focused ultrasound prostate-specific antigen (PSA) nadir [blue line, area under the curve (AUC) 0.87] and pre-biopsy PSA (green line, AUC 0.95).

As focal therapy for prostate cancer has advanced there is a growing need for imaging-based disease assessment, and MRI is increasingly employed [7]. In addition to merely detecting disease presence, MRI offers the promise of identifying the size and location of cancers [15]. Conversely, using PSA levels to detect residual disease after focal therapy is likely to be more difficult as PSA does not fall to zero and small changes resultant from residual disease may be masked by PSA produced from the remaining prostate.

Our study investigated DCE-MRI detection of biopsy-confirmed residual disease following whole-gland HIFU, and compared the accuracy of DCE-MRI against PSA measurement.

The study population comprised a mixture of patients biopsied for an elevated or rising post-HIFU PSA and individuals enrolled onto a prospectively running clinical trial in which biopsy was performed irrespective of PSA level. Within this population we found a 57% rate of residual or recurrent disease, higher than previously reported studies [4]. However, this is not unexpected given the selection bias in this retrospective study towards patients with an increased likelihood of residual disease. Indeed, the aim of our study was to assess the performance of DCE-MRI for detection of residual disease and not to determine recurrence rate following HIFU *per se*; and a population enriched with residual disease is better suited to our study aim.

The primary finding of our study confirms that PSA measurement has a high sensitivity and specificity for detection of residual disease following whole-gland HIFU. This is consistent with several previous studies, which have correlated PSA nadir with outcome [16, 17]. The results suggest that regular measurement of PSA levels will detect most residual or recurrent disease following whole-gland HIFU.

It is perhaps not surprising that the post-HIFU pre-biopsy PSA was more predictive of residual disease than the post-HIFU PSA nadir, as it is likely that small volume residual disease may have grown in the interval between HIFU treatment (and associated PSA nadir) and biopsy. We also cannot exclude the possibility that this finding is due to patient selection bias. As described earlier, approximately 50% of patients identified for inclusion within this study had post-HIFU biopsy performed consequent to a high or rising PSA, and this may have increased the sensitivity and specificity of PSA threshold findings. Nevertheless, our results support the standard practice of surveillance of the patient after treatment by PSA measurement.

Our second major finding was that sensitivity of MRI for detection of residual disease ranged from 73 to 87%, and specificity from 73 to 82%, with good agreement between readers. Previously, Kim et al [6] have examined the ability of contrast-enhanced MRI to predict biopsy results in a group of patients treated with a
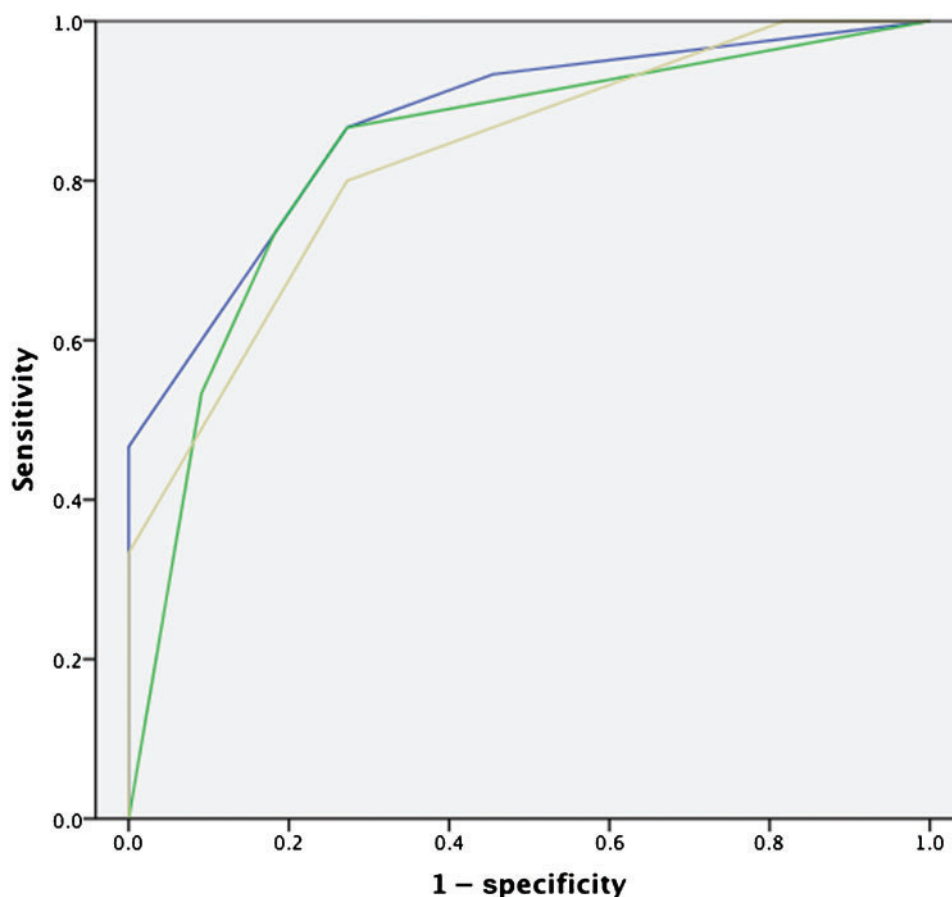
Figure 6. Dynamic contrast-enhanced MRI receiver operating characteristic curves for Readers 1 [blue line, area under the curve (AUC) 0.87], 2 (yellow line, AUC 0.83) and 3 (green line, AUC 0.83).

different HIFU device (Ablatherm) and suspected of having residual disease. They used T_2 weighted images, dynamic contrast enhancement and diffusion-weighted imaging. They reported a sensitivity of 80–87%, and a specificity of 63–68% for detection of disease using contrast-enhanced MRI [6], which is in keeping with our overall DCE-MRI sensitivity and specificity of 73%.

We were unable to demonstrate a significant difference between the ability of PSA threshold values and MRI readers' assessments of DCE images for detection of residual tumour. Although our results suggest that MRI adds little to the use of PSA in the routine monitoring of patients for residual or recurrent disease after HIFU, it has the fundamental advantage that it may be used to localise the tumour. Indeed, Rouvière et al [10] have recently shown that biopsies targeted to areas of suspicion on post-HIFU (Ablatherm device) DCE-MRI were 3.35 times more likely to be positive for tumour than untargeted cores [11].

We deliberately did not investigate tumour localisation with MRI, and performed analysis on the whole-gland level. While division of the residual post-HIFU prostate into quadrants would have increased data for analysis, this may overestimate specificity of DCE-MRI on a *per patient* level [18]. Our results are therefore more likely to represent the true clinical performance of MRI for disease detection.

Our study does have limitations. First, although histological evidence of disease presence or absence was available for each patient and the post-HIFU

prostate is of low volume, tumour may still have been missed on the transrectal biopsy used as a reference standard for our study [19].

Furthermore, as evaluation of post-HIFU DCE-MRI is in its infancy our readers were relatively inexperienced, potentially resulting in the slight underperformance of DCE-MRI compared with PSA as a method of detecting residual disease. However, all readers were experienced in pre-treatment prostate MRI reporting and were given a standard 1 h tuition as described in the Materials and methods; furthermore, our reported DCE-MRI performance was in keeping with previous studies [6].

In summary, our study has shown that DCE-MRI performed following whole-gland HIFU (Sonablate 500 device) for detection of residual disease has sensitivity and specificity similar to traditionally employed PSA measurements. Our findings support the current post-HIFU patient management strategy of: surveillance with serial PSA measurement and then, in case of biochemical recurrence, use of MRI to detect the local recurrence and guide biopsy. Finally, we believe that with increasing use of focal therapies the accuracy of serial PSA as a surveillance test is likely to worsen, and here in particular DCE-MRI may offer an alternative surveillance method.

Acknowledgments

Conflicts of interest

M Emberton has acted as a paid consultant to Misonix Inc. (the European distributors of the Sonablate device) and also received honoraria for training and teaching. H Ahmed has received travel grants from Misonix Inc. and acted as a paid trainer for UK HIFU with the Sonablate device.

References

1. Blana A, Walter B, Rogenhofer S, Wieland WF. High-intensity focused ultrasound for the treatment of localized prostate cancer: 5-year experience. Urology 2004;63: 297–300.
2. Colombel M, Gelet A. Principles and results of high-intensity focused ultrasound for localized prostate cancer. Prostate Cancer Prostatic Dis 2004;7:289–94.
3. Shoji S, Nakano M, Nagata Y, Usui Y, Terachi T, Uchida T. Quality of life following high-intensity focused ultrasound for the treatment of localized prostate cancer: a prospective study. Int J Urol 2010;17:715–19.
4. Blana A, Murat FJ, Walter B, Thuroff S, Wieland WF, Chaussy C, et al. First analysis of the long-term results with transrectal HIFU in patients with localised prostate cancer. Eur Urol 2008;53:1194–201.
5. Riviere J, Bernhard JC, Robert G, Wallerand H, Deti E, Maurice-Tison S, et al. Salvage radiotherapy after high-intensity focussed ultrasound for recurrent localised prostate cancer. Eur Urol 2010;58:567–73.
6. Kim CK, Park BK, Lee HM, Kim SS, Kim E. MRI techniques for prediction of local tumor progression after high-intensity focused ultrasonic ablation of prostate cancer. AJR Am J Roentgenol 2008;190:1180–6.
7. Polascik TJ, Mouraviev V. Focal therapy for prostate cancer is a reasonable treatment option in properly selected patients. Urology 2009;74:726–30.
8. Villers A, Puech P, Mouton D, Leroy X, Ballereau C, Lemaitre L. Dynamic contrast enhanced, pelvic phased array magnetic resonance imaging of localized prostate cancer for predicting tumor volume: correlation with radical prostatectomy findings. J Urol 2006;176:2432–7.
9. Haider MA, Chung P, Sweet J, Toi A, Jhaveri K, Menard C, et al. Dynamic contrast-enhanced magnetic resonance imaging for localization of recurrent prostate cancer after external beam radiotherapy. Int J Radiat Oncol Biol Phys 2008;70:425–30.
10. Rouvière O, Girouin N, Glas L, Ben Cheikh A, Gelet A, Mège-Lechevallier F, et al. Prostate cancer transrectal HIFU ablation: detection of local recurrences using T_2-weighted and dynamic contrast-enhanced MRI. Eur Radiol 2010; 20:48–55.
11. Illing RO, Leslie TA, Kennedy JE, Calleary JG, Ogden CW, Emberton M. Visually directed high-intensity focused ultrasound for organ-confined prostate cancer: a proposed standard for the conduct of therapy. BJU Int 2006;98: 1187–92.
12. Kirkham APS, Emberton M, Hoh IM, Illing RO, Freeman AA, Allen C. MR imaging of prostate after treatment with high-intensity focused ultrasound. Radiology 2008;246: 833–44.
13. Fleiss JL. Statistical methods for rates and proportions. Chichester, UK: Wiley; 1981.
14. Hanley JA, McNeil BJ. A method of comparing the areas under receiver operating characteristic curves derived from the same cases. Radiology 1983;148:839–43.
15. Mazaheri Y, Shukla-Dave A, Muellner A, Hricak H. MR imaging of the prostate in clinical practice. MAGMA 2008; 21:379–92.
16. Blana A, Brown SCW, Chaussy C, Conti GN, Eastham JA, Ganzer R, et al. High-intensity focused ultrasound for prostate cancer: comparative definitions of biochemical failure. BJU Int 2009;104:1058–62.
17. Uchida T, Illing RO, Cathcart PJ, Emberton M. To what extent does the prostate-specific antigen nadir predict subsequent treatment failure after transrectal high-intensity focused ultrasound therapy for presumed localized adenocarcinoma of the prostate? BJU Int 2006;98:537–9.
18. Kirkham APS, Emberton M, Allen C. How good is MRI at detecting and characterising cancer within the prostate? Eur Urol 2006;50:1163–74.
19. Djavan B, Ravery V, Zlotta A, Dobronski P, Dobrovits M, Fakhari M, et al. Prospective evaluation of prostate cancer detected on biopsies 1, 2, 3 and 4: when should we stop? J Urol 2001;166:1679–83.